

# Monitoring of Breath Sound under Daily Environment by Ceiling Dome Microphone

Yoshifumi NISHIDA, Toshio HORI, Takashi SUEHIRO, and Shigeoki HIRAI  
Intelligent Systems Division, Electrotechnical Laboratory

## Abstract

This paper proposes a new method for monitoring normal breath sounds in our daily environment where many kinds of noise exist. In a typical conventional breath monitor, a thermistor, an accelerometer, or a contact-type microphone must be attached directly to the person's body such as near the nose and the mouth, or over the chest wall and the trachea. This paper focuses on key issues stemming from a factor of the environment; extraction of breath sounds from sensor signals contaminated by environmental noise, and the realization of a monitoring system suitable for our homes. The features of normal breath sounds were clarified by frequency analysis. Based on the features, a method for extracting normal breath sounds is discussed. This paper also describes a ceiling dome microphone, which is a kind of a parabolic sound concentrator. It has a function of detecting normal breathing sounds with high sensitivity while keeping the room's appearance natural. The gain obtained by such a concentrator is analyzed theoretically from an acoustic point of view. Experimental results confirmed the feasibility of the proposed method.

## 1 Introduction

Daily personal healthcare at home is a topic of great concern recently. Continuous monitoring of a person's physiological status by him or herself is required. An unrestrained and non-invasive means of observing physiological status is the key technology to realize it. Visual, tactile, and/or auditory sensors are quite suitable for this purpose.

The authors are experienced in conducting clinical studies for monitoring respiratory conditions of a patient with the help of doctors at a hospital. The human respiratory system is very complex and understandably requires monitoring with many sensors such as pressure sensors to monitor the chest and abdomen's movement, thermistor for airflow around the

nose and mouth, a contact-type of microphone for snoring, oximeters for oxygen saturation, and mercury sensors for posture. Indeed, these sensors can monitor physiological values certainly as long as they are used adequately. Actually, however, they very often fail to monitor continuously. For example, in 48 percent of the cases (21 of 43 cases) in the clinical study the authors conducted, the monitoring system failed to measure the physiological values continuously enough to diagnose disease. This suggests that even in a hospital where more priority is given to accurate monitoring than to comfortable monitoring, unrestrained monitoring is required to minimize this failure.

The aim of this paper is to propose a new method for monitoring normal breath sounds in a daily environment where many kinds of noise exist. This method has the possibility of use for monitoring respiratory airflow in place of a conventional airflow monitor such as a thermistor, an accelerometer, or a contact-type of microphone.

This paper focuses on key issues stemming from a factor of the environment; 1) extraction of breath sounds from sensor signals contaminated by environmental noise, and 2) realization of a monitoring system suitable for use in our homes.

As for 1), in Section 2, the spectral characteristics of normal breath sounds are clarified and a method for detecting the sounds is discussed.

Frequency analysis of breath sounds has been attempted by a number of researchers. In particular, Gavriely et al. accurately characterized normal breath sounds and wheezing breath sounds[1, 2]. They used a contact-type of microphone which had a useful frequency response in the range of 0.02[Hz] to 2[kHz], and attached it to the subject's body over the chest wall and the trachea. In contrast, the authors characterize normal breath sounds which are emitted from the nose and propagate in the air, using a condenser microphone whose useful frequency response ranges from 30[Hz] to 100[kHz].

As for 2), a ceiling dome microphone, a kind of a

parabolic sound collector, is presented in Section 3. The gain obtained by the microphone is analyzed theoretically from an acoustic point of view.

## 2 Normal Breath Sounds

Figure 1 shows the spectral distribution of normal breath sounds measured in an environment where the noise level is 38.5[dB(A)]. The normal breath sounds were measured at a distance of 100[mm] from the subject's nose. The microphone used is a non-directional 1/4-inch condenser microphone which has a useful frequency response in the range of 30[Hz] to 100[kHz]. Its sensitivity is  $-48$ [dBreV/Pa]. In the figure, the gray area indicates normal breath sounds and the white area indicates background noise. This figure shows that normal breath sounds include a wide range of frequencies in an audio range.

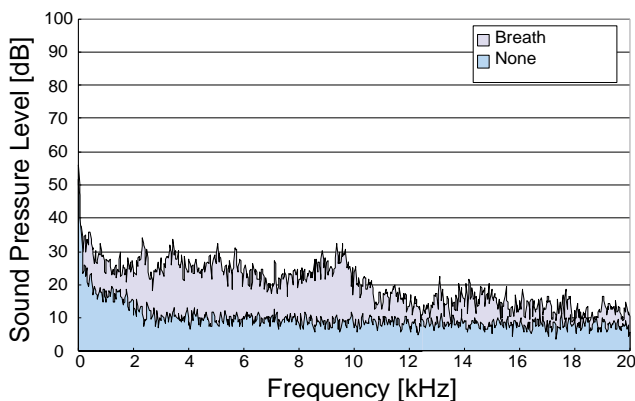


Fig. 1: Spectral characteristics of normal breath sounds (0 to 20[kHz])

In Fig. 2 noises generated by such sound sources as an air conditioner, an air cleaner, a refrigerator, a telephone, a TV, and a computer are superimposed on Fig. 1. These sounds were measured at a distance of 100[mm]. The white area indicates the noises from these devices. The figure shows that compared with normal breath sounds, noises generated by these devices have relatively limited and unique frequency distribution patterns. This indicates that it is possible to detect normal breath sounds by selecting the range where signal-to-noise ratio is high, and in the case of our environment, the range is 5 to 15[kHz].

Figure 3 shows the spectral distribution of normal breath sounds, deep breath sounds, and other back-

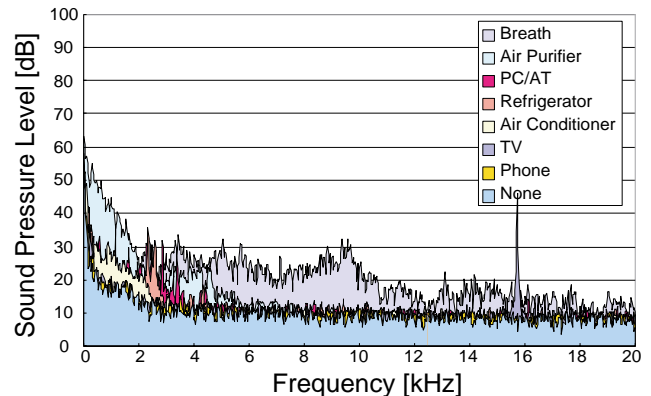


Fig. 2: Comparison between normal breath sounds and background noise (0 to 20[kHz])

ground noises in the range of 0 to 100[kHz]. This figure indicates that the frequency of deep breath sounds reaches an ultrasonic range. The maximum frequency is around 50[kHz]. In the figure, the two noises whose sound pressure level is about 40[dB] at 28[kHz] and 56[kHz] come from a PC/AT computer.

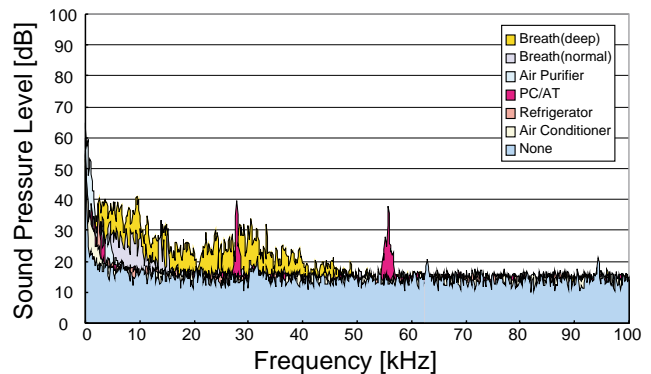


Fig. 3: Comparison among normal breath sounds, deep breath sounds, and background noise (0 to 100[kHz])

Based on the above analysis, let us consider a method for detecting normal breath sounds. In general, the intensity of sound is proportional to  $1/r^2$  in the free sound field, where  $r$  denotes the distance from the sound source. Since the sound pressure level (SPL) in decibel of normal breath sounds is at most 30[dB] at a distance of 100[mm] from the source, if normal breath sounds are measured at a distance of 1,000[mm], the

SPL of normal breath sounds falls 20[dB] to 10[dB], which is equal to the SPL of background noise, and then it becomes impossible to detect normal breath sounds. This means that measuring the high-frequency content of normal breath sounds is not enough to identify normal breath sounds. To detect normal breath sounds, it is necessary to measure the sounds at a position close to the source or at a position relatively distant from the source using a directional microphone. The authors deal with a method for detecting breath sounds using a directional microphone in the next section.

### 3 Ceiling Dome Microphone

To detect the only sound that comes from a certain direction, we can utilize a super-directional microphone such as a microphone array[3], a reflector type of microphone (typically, a parabolic sound collector), or a line microphone. Generally speaking, if the microphones are the same in the characteristic length, the resulting sensitivity is also the same even if their measuring principles are different. The reflector type of microphone realizes high sensitivity easily without complex signal processing. This study adopts this type of microphone for detecting breath sounds.

A parabolic, elliptical, or spherical concave is used for the sound reflector. While a parabolic reflector is suitable for collecting a plane wave, that is to say when the sound source is far from the reflector, an elliptical one is suitable when a sound source is emitted from a point and is near the reflector. However their sensitivities are not very different from each other. Considering that a spherical concave which is widely used for a ceiling dome is applicable for use as a sound reflector, and that such a sound reflector can be embedded into the living space as interior decoration, this paper deals with a spherical sound reflector and discusses sound concentration using it.

#### 3.1 System configuration and outline of specification

The authors constructed a ceiling dome microphone which consists of the ceiling dome for a sound reflector, a condenser microphone, a lighting fixture, and a host computer. Figure 4 shows a photograph of the room with the ceiling dome microphone installed and Fig. 5 shows a photograph of the ceiling dome microphone.

This device has two functions: indirect lighting and collecting sound. The ceiling dome is used to reflect



Fig. 4: Room with ceiling dome microphone installed

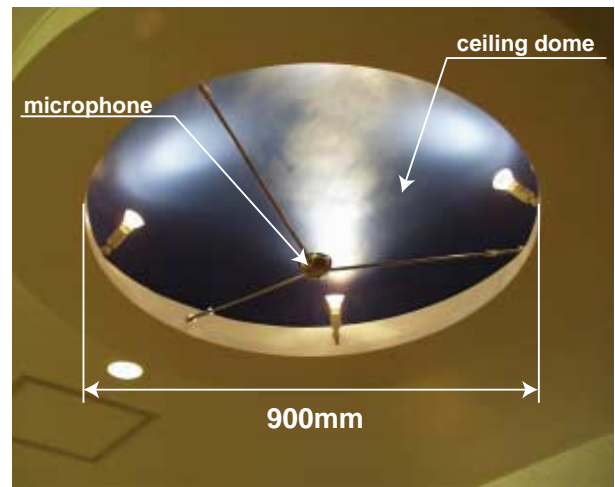


Fig. 5: Ceiling dome microphone

both light and sound. The microphone is set at the acoustic focal point of the reflector. The microphone is non-directional in hemisphere and its frequency response is almost flat between 30 to 20,000[Hz]. Its sensitivity is  $-42[\text{dBreV/Pa}]$ . The device can detect sound coming from a certain direction with high sensitivity while keeping the room's appearance natural. In our room, it is positioned above the bed to detect breath sounds during sleep. The gain obtained by the

ceiling dome ranges from  $-18$  to  $31$  [dB] depending on frequency of sound. The radius of curvature is  $775$ [mm]. The diameter of the dome is  $900$ [mm]. The host computer samples output from the microphone via an AD converter at  $40$ [kHz].

Theoretical analysis on sound concentration caused by the ceiling dome is described in Section 3.2.1. The experimental results are reported in detail in Section 3.2.2.

## 3.2 Theoretical analysis of sound concentration due to spherical concave

### 3.2.1 Theory of sound concentration

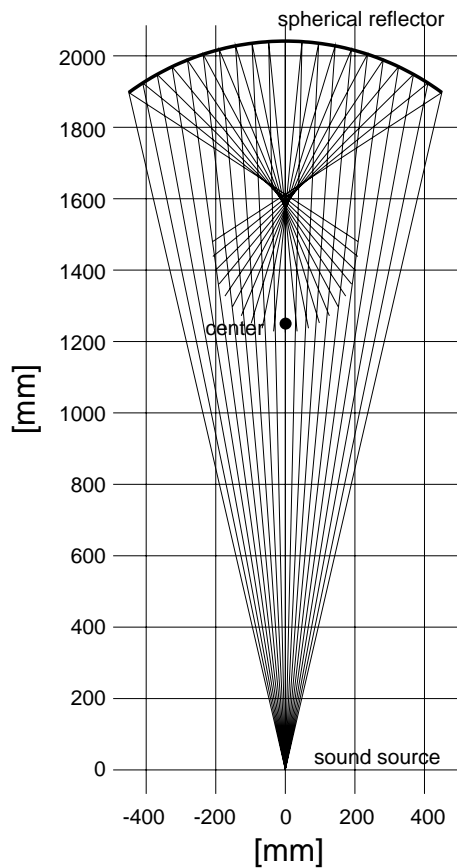


Fig. 6: Sound concentration by spherical concave

Figure 6 shows the reflection of a sound wave by a spherical concave. The sound source is assumed to be a single sound source. In this figure the size of the concave and the distance between the concave and the sound source are the same as those of the actual con-

ditions we used. Although we can see the acoustic focus roughly from the figure, it is unclear whether it is an apparent acoustic focus or the real one because this sound reflection model is based on geometrical acoustics. In geometrical acoustics, the phase difference resulting from the difference in the length of propagation courses of the sound rays is not considered. Accordingly, we cannot discuss the effect of frequency on sound concentration. This paper analyzes sound concentration theoretically using a wave equation.

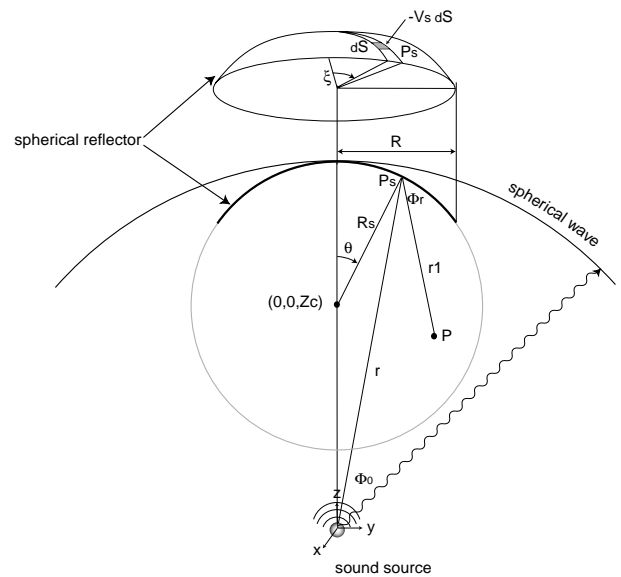


Fig. 7: Model of sound reflection by spherical concave

Figure 7 defines the variables that describe the reflector, sound source, and other points. It is assumed that the sound source is a single sound source and that the reflector is a spherical concave. The reflection coefficient on the reflector is assumed to be 1.0.

In the absence of a reflector, the velocity potential  $\dot{\Phi}_s$  at a point  $P_s$  on the reflector is expressed by

$$\dot{\Phi}_s = \frac{U_0}{4\pi r} e^{-jkr}, \quad (1)$$

where  $U_0$ ,  $k$  and  $r$  denote the volume velocity of the sound source, the wave number of the sound wave, and the distance of  $P_s$  from the sound source.

Then, the particle velocity  $\dot{V}_s$  at  $P_s$  becomes

$$\begin{aligned} \dot{V}_s &= -\frac{\partial \dot{\Phi}_s}{\partial r} \\ &= \frac{U_0(1 + jkr)}{r^2} e^{-jkr}. \end{aligned}$$

If  $kr \gg 1$ , we may write

$$\dot{V}_s = \frac{jkU_0}{4\pi r} e^{-jkr}. \quad (2)$$

If the reflector is placed in this sound field and it does not vibrate, the particle velocity  $\dot{V}_s$  becomes 0. This means that the velocity potential generated by the reflected wave can be considered to be that generated by the reflector vibrating at particle velocity  $-\dot{V}_s$ .

According to Rayleigh's theory[5], when the only small element  $dS$  situated at  $P_s$  vibrates at volume velocity  $-\dot{V}_s \cdot dS$  and the rest does not vibrate, the velocity potential caused by the element  $dS$  is expressed by

$$d\dot{\Phi}_r = -\frac{\dot{V}_s e^{-jkr_1}}{2\pi r_1} dS,$$

where  $r_1$  denotes the distance of a point  $P$  from  $P_s$  which is the position of the element  $dS$ . The velocity potential from the whole reflector is obtained by integrating  $d\dot{\Phi}_r$ . Thus

$$\dot{\Phi}_r = \int d\dot{\Phi}_r = -\int \frac{\dot{V}_s e^{-jkr_1}}{2\pi r_1} dS, \quad (3)$$

from which, by eliminating  $\dot{V}_s$  using Eq. (2), we obtain

$$\dot{\Phi}_r = -\int \frac{jkU_0 e^{-jk(r+r_1)}}{8\pi^2 r \cdot r_1} dS.$$

Hence, the sound pressure  $\dot{P}_r$  at  $P$  becomes

$$\begin{aligned} \dot{P}_r &= j\omega\rho\dot{\Phi}_r \\ &= \int \frac{k\rho\omega U_0 e^{-jk(r+r_1)}}{8\pi^2 r \cdot r_1} dS, \end{aligned} \quad (4)$$

where  $\omega$  is the angular velocity, and  $\rho$  is the density of air. Note that  $r$  and  $r_1$  change in accordance with the position of the element  $dS$ .

To prepare for numerical analysis, we must digitize Eq. (4). If the position of the sound source lies in the origin and  $P_s$  is expressed by

$$P_s = (R_s \sin \theta \cos \xi, R_s \sin \theta \sin \xi, R_s \cos \theta + Z_c),$$

$dS$  can be replaced by

$$\Delta S = R_s^2 \sin \theta \Delta \xi \Delta \theta,$$

and Eq. (4) is digitized as follows.

$$\dot{P}_r = \frac{k\rho\omega U_0 R_s^2}{8\pi^2} \sum \sum \frac{e^{-jk(r_i+r_{1i})}}{r_i \cdot r_{1i}} \sin \theta \Delta \xi \Delta \theta$$

In the above equation, if  $\Delta \xi \Delta \theta$  is constant, we obtain

$$\begin{aligned} |\dot{P}_r| &= \frac{k\rho\omega U_0 R_s^2 \Delta \xi \Delta \theta}{8\pi^2} \sqrt{(\sum \sum \frac{\sin \theta}{r_i \cdot r_{1i}} \cos(k(r_i + r_{1i})))^2} \\ &\quad + (\sum \sum \frac{\sin \theta}{r_i \cdot r_{1i}} \sin(k(r_i + r_{1i})))^2. \end{aligned} \quad (5)$$

$(r_i = |P_s^i|, r_{1i} = |P_s P^i|)$

Using Eq. (5), we can calculate the sound pressure distribution by changing the position of  $P$  to find the theoretical acoustic focus.

### 3.2.2 Results of numerical analysis

Figure 8 shows the gain obtained by the ceiling dome. The vertical axis indicates

$$Gain = 20 \log \frac{P_1}{P_0} \quad [dB], \quad (6)$$

where  $P_1$  denotes the sound pressure at an acoustic focus (0,0,1.56)[m] and  $P_0$  denotes the sound pressure at the same position without the ceiling dome. The position of the sound source is (0,0,0)[m]. In the figure, the dots express measured values. The line expresses theoretical values. The theoretical values were calculated using Eq. (5).

From the figure, we can see that the gain increases gradually, and that the measured values correspond to the theoretical ones considerably although the measured values are a little less than the theoretical ones. This means that the fundamental theory of acoustics can be used to explain the acoustic features of a spherical sound reflector. The same theory would be applicable to other kinds of concave reflectors.

From the figure, we can see that the gain is maintained at more than 20[dB] for high frequency sounds of more than 6[kHz]. Since in normal breath sounds the signal-to-noise ratio is high in the range of 5 to 15[kHz], the ceiling dome microphone is suitable for detecting normal breath sounds.

Figure 9 depicts sound fields near the dome when frequency is 500[Hz] to 40[kHz]. Each sound field is solved by numerical calculation using Eq. (5). The vertical axis indicates the height from the center of the curvature of the dome. The figure shows that the acoustic focal point moves as the frequency changes. To be precise, in an audio region, the acoustic focal point is not coincident to that calculated by geometrical acoustic method. However, as the frequency becomes higher, the acoustic focus becomes closer to the geometrical acoustic focus as shown in Fig. 10. The geometrical acoustic focus is calculated by sound ray tracing method[4].

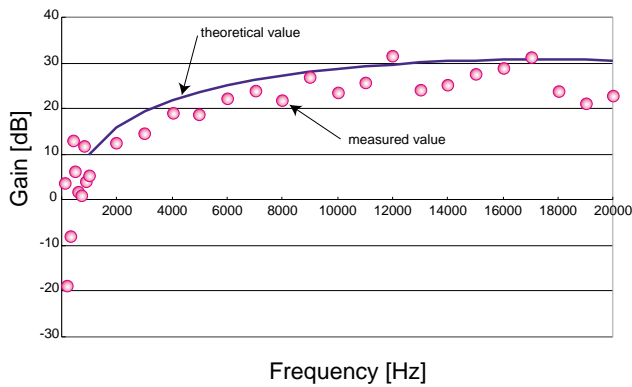


Fig. 8: Gain from ceiling dome microphone (comparison between measured and theoretical values)

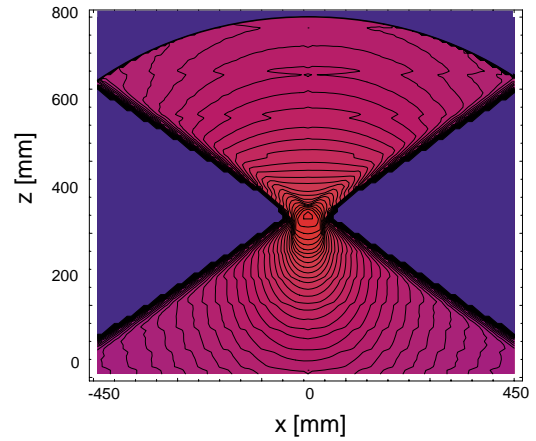


Fig. 10: Sound field solved by geometrical acoustics method

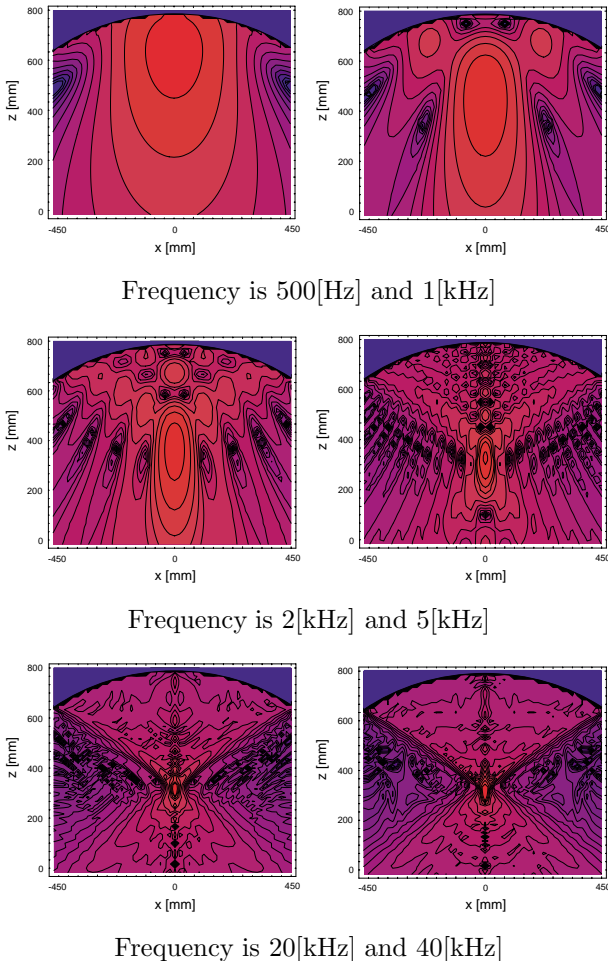


Fig. 9: Sound field near ceiling dome when the frequency is 500[Hz] to 40[kHz]

Let us consider the calculation of the directional pattern of the dome ceiling. According to Helmholtz's theorem of reciprocity, the sound pressure at focal point A  $((0, 0, 1.56)[m])$  given by a sound source situated at another point B is the same as the sound pressure at point B given by a sound source situated at point A. Therefore, to calculate the directional pattern using Eq. (5), we have only to calculate the pressure distribution near  $(0,0,0)$  when the sound source exists in the focus. Figure 11 shows the directional pattern of the dome ceiling microphone around the sound source situated at  $(0,0,0)$ . While the ceiling dome microphone has little directivity for low frequency sounds of less than 1[kHz], it has sharp directivity for high-frequency sounds of more than 5[kHz].

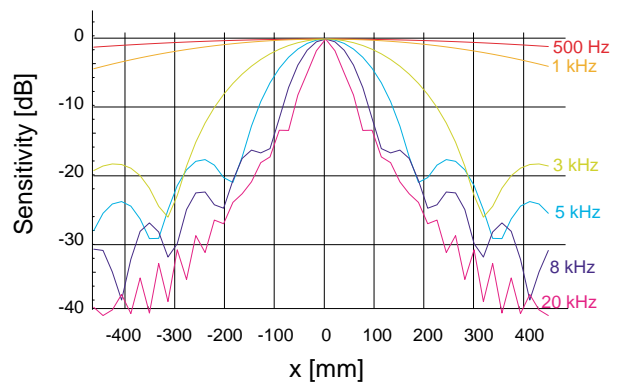


Fig. 11: Theoretical value of directional pattern

## 4 Detection of Normal Breath Sounds by Ceiling Dome Microphone

Figure 12 shows the experimental results of detecting normal breath sounds using the ceiling dome microphone. The experiment was conducted in an environment where the noise level is 46.5[dB(A)]. The measurement was taken at a distance of 2,040[m] from the subject's nose. In the figure, (a) is the integral of the power spectra of the measured sounds from 0 to 20[kHz], (c) is the integral of the power spectra from 5 to 15[kHz], (b) is the integral of the power spectra of background noises without the ceiling dome, and (d) is the integral of the power spectra of background noises when the ceiling dome exists. The results of (a) and (c) show that the integration in the region where the signal-to-noise ratio is high is effective for detecting normal breath sounds. The results of (b) and (d) indicate the dome ceiling has an effect of reducing the background noise level.

Figure 13 shows the experimental results of detecting normal breath sounds when the subject is in supine, lateral, and prone positions. The top figure explains that normal breath sounds consist of inhalation sounds and exhalation sounds. These figures show that it is possible to detect normal breath sounds irrespective of the subject's posture.

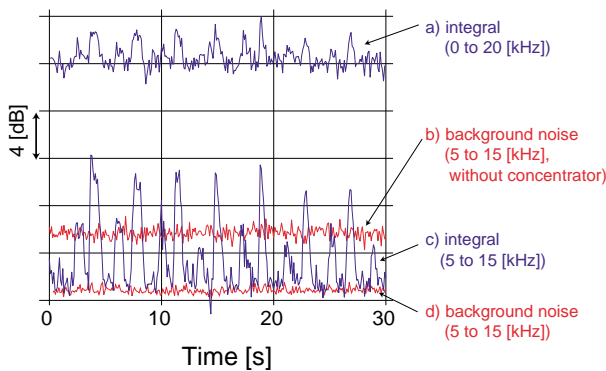


Fig. 12: Experimental results of breath sound detection

## 5 Conclusion

This paper proposed a new method for detecting normal breath sounds. By frequency analysis, the au-

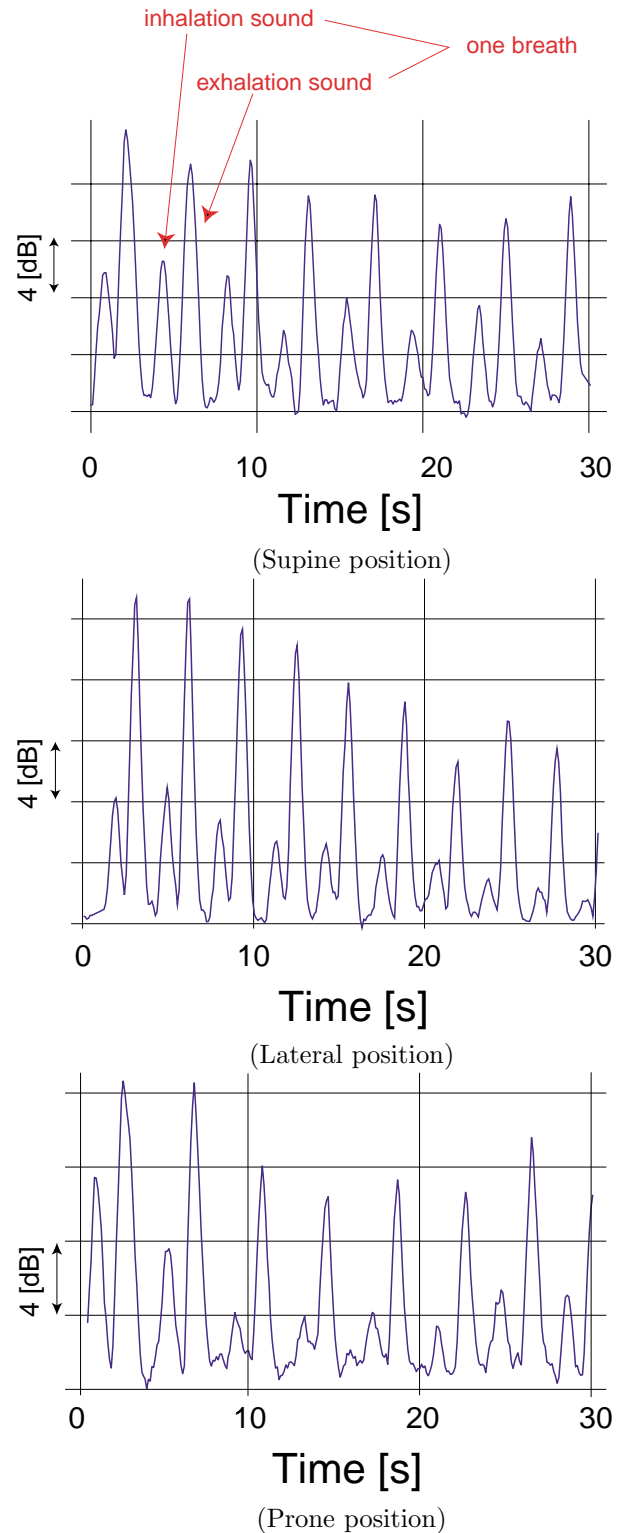


Fig. 13: Detection of breath sounds when subject is in supine, lateral, and prone positions

thors characterized normal breath sounds in comparison with background noise: 1) Breath sounds have a wide range of frequencies in the audio range, 2) Electric appliances in the home have a relatively limited and low range of frequencies, and in many appliances, the frequency is less than 5[kHz], and 3) the signal-to-noise ratio is high in the range of 5 to 15[kHz].

This paper introduced a ceiling dome microphone, a new device for collecting normal breath sounds while keeping the room's appearance natural. From an acoustic point of view, the authors discussed its frequency response theoretically. The fundamental results of the frequency response showed that the ceiling dome microphone constructed by the authors can maintain a gain of more than 20[dB] for high-frequency sounds of 6 to 20[kHz].

Finally, the authors demonstrated their proposed method experimentally using an actual ceiling dome microphone. The experimental results confirmed the effectiveness of the method and the feasibility of the function in a home environment.

In future studies, applying this method to more subjects including patients to clarify differences among individuals is deemed necessary.

## Acknowledgments

We would like to thank Sojun Sato of the Metrology Fundamentals Division in the Electrotechnical Laboratory for his useful suggestions on acoustics analysis. This study was funded in part by a Grant-in-Aid from The Fluidity Promotion Research System of the Science and Technology Agency of Japan.

## References

- [1] N. Gavriely, Y. Palti, G. Alroy, "Spectral Characteristics of Normal Breath Sounds," *Journal of Applied Physiology: Respiratory, Environment and Exercise Physiology*, Vol. 50, No. 2, pp307-314, 1981
- [2] N. Gavriely, Y. Palti, G. Alroy, J.B. Grotberg, "Measurement and Theory of Wheezing Breath Sounds," *Journal of Applied Physiology: Respiratory, Environment and Exercise Physiology*, Vol. 57, No. 2, pp481-492, 1984
- [3] Y. Kaneda, J. Ohga: "Adaptive Microphone-array System for Noise Reduction," *IEEE Trans. Acoust. Speech & Signal Process.*, Vol. ASSP-34, No. 6, pp1391-1400, 1986
- [4] A. Krokstad, "Algorithmic Representation of the Ray Tracing Technique," *Applied Acoustics*, 18, pp449-469, 1985
- [5] J.W.S. Rayleigh, *The Theory of Sound*, Vol. 2, Dover Publications (New York), (original) 1877, (reprint) 1945